The Radio Science Bulletin

ISSN 1024-4530

INTERNATIONAL
UNION OF
RADIO SCIENCE

UNION
RADIO-SCIENTIFIQUE
INTERNATIONALE

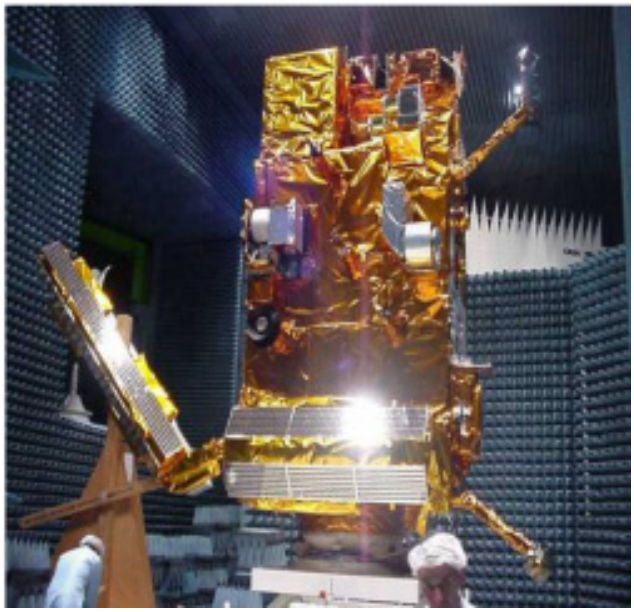

No 328
March 2009

URSI, c/o Ghent University (INTEC)
St.-Pietersnieuwstraat 41, B-9000 Gent (Belgium)

Contents

Front cover: EMC testing of the METOP EQM spacecraft. See paper by A. Ciccolella and F. Marliani pp. 9-19.

For information, please contact :
The URSI Secretariat
c/o Ghent University (INTEC)
Sint-Pietersnieuwstraat 41, B-9000 Gent, Belgium
Tel.: (32) 9-264 33 20, Fax: (32) 9-264 42 88
E-mail: info@ursi.org
http://www.ursi.org

Characterizing the Lower Ionosphere with a Space - Weather - Aware Receiver Matrix

D.D. Rice
R.D. Hunsucker
J.V. Eccles
J.J. Sojka
J.W. Raitt
J.J. Brady

Abstract

Current ionospheric models are very good at specifying regular diurnal and seasonal variations of the E and F regions of the ionosphere. Less is known about the behavior of the D region, although progress has recently been made with models such as the Data-Driven D-Region (DDDR). However, significant departures from modeled behaviors are observed even during solar minimum conditions, due to complex ionospheric weather effects arising from both solar activity above and terrestrial atmospheric perturbations below. The D-region perturbations directly affect VLF communications, and also affect daytime absorption of frequencies from LF through HF. Perturbations in the E and F regions affect HF propagation, and may impact transionospheric communications at much higher frequencies.

In order to characterize ionospheric weather and its effects on operational systems, better observing networks are needed, comparable to those utilized to study and forecast mesoscale (10-1000 km) tropospheric weather. Current terrestrial observatories used in space-weather studies are widely separated geographically. They often do not record continuous observations, making it difficult to quantify the spatial and temporal behavior of space-weather phenomena.

We describe a passive sensor network designed to map conditions in the D and E regions and in the F-region bottomside on a continental scale, based on continuous monitoring of propagation effects on signal strength in the VLF through HF frequency range (10 kHz to 30 MHz.) This network is inexpensive to build and to operate, providing information about ionospheric conditions along the monitored signal paths, and enabling space weather effects to be inferred. This weather information is used to update mesoscale D- and E-region models, which are in turn used by radio-propagation modeling tools to analyze signal observations.

A prototype network has been deployed in the western United States, with six fixed and two transportable sensors. Data from the prototype and from an earlier HF-only experiment show that D-region variability, sporadic E, and bounds on F-region parameters can be inferred. When used in conjunction with existing ionospheric observatory data, this sensor network offers an affordable means of studying mesoscale D- and E-region weather patterns, with excellent temporal resolution (a few minutes) over entire solar cycles.

1. Introduction

The terrestrial ionosphere has been studied for decades, and much progress has been made in understanding the mechanisms and climatology of the ionosphere. The focus has been primarily on the E and F regions, since they are easily explored by remote-sensing methods, such as radars and ionosondes; the F region is also accessible to in situ satellite measurements. The E and F regions are responsible for the long-distance radio propagation that was the focus of early studies. Later studies have been motivated by the impact these regions have on space vehicles, through effects such as drag and charging.

D-region processes are less well understood. The D region forms the top of the Earth-ionosphere waveguide that defines propagation at very low frequencies (< 100 kHz),

D. D. Rice, J. V. Eccles, J. J. Sojka, J. W. Raitt, and J. J. Brady are with Space Environment Corporation, 221 N. Spring Creek Parkway, Suite A, Providence, Utah 84332-9791 USA; Tel: +1 (435) 752-6567; Fax: +1 (435) 752-6687; E-mail: Don.Rice@spacenv.com. R. D. Hunsucker is with RP Consultants, 7917 Gearhart Street, Klamath Falls, OR 97601 USA; E-mail: rdhrpc1@charter.net.

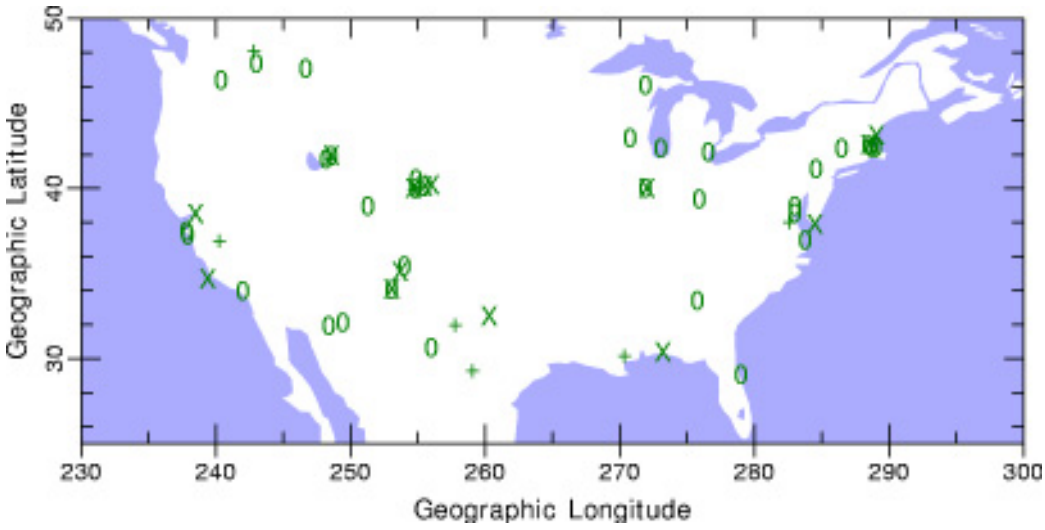

Figure 1.The distribution of magnetometers (+), optical instruments (O), and ionosondes/radars (X) in the contiguous United States from the CEDAR database.

and causes significant daytime absorption for frequencies below about 15 MHz. Few measurement techniques used for E- and F-region studies are applicable at D-region heights. Most exploration has been done with short sounding-rocket campaigns, certain satellite instruments, lidars, and specialized radars (see, for example, [1]). Mesospheric studies have provided more information about this region in recent years, but the lack of long-term, wide-area observational data hampers efforts to create realistic models.

Currently, the modeling and prediction of space-weather impacts on radio propagation are based almost entirely on statistical climatology. Mesoscale descriptions of D- and E-region responses to space weather are not available in a timely manner during the disturbances from either observations or models. Communicators need such information covering ranges of hundreds to thousands of kilometers, in order to provide effective long- and short-distance communications. This study and the proposed observation network address these needs.

The potential impacts of space weather on communications are well known. Storm effects have been described in some detail by Davies [2, Chapter 9], and Hunsucker and Hargreaves [3, Chapter 8]. Specific effects of interest in this study are:

- Sudden ionospheric disturbances (SIDs) at VLF, associated with solar X-ray flares, cause dramatic shifts in the amplitude and phase of signals used for naval communications and navigation aids [4]. At HF, X-ray flares cause strong absorption that may black out communication links for hours.
- Nitric oxide (NO) transport between high and mid-latitudes with planetary wave scales are associated with increased winter daytime D-region absorption at lower HF frequencies [5, 6], and may cause subtle VLF propagation effects.
- Sporadic E – remarkably thin, dense layers at E-region altitudes – allows signals at frequencies well above the normal maximum-usable frequency (MUF) to propagate over large distances. Generally believed to be due to wind shears [7], sporadic E may be affected by planetary waves and tides [8].

A fundamental problem with studies of space-weather phenomena is that observations are widely separated in space. Observations are often incomplete in time, with the larger instruments such as incoherent-scatter radars operating only occasionally in campaign modes. Figure 1 shows the distribution of ionospheric instrumentation in the contiguous United States, listed in the CEDAR database. Sojka et al. [9] argued that the existing observatories cannot answer long-standing questions about space-weather and upper-atmosphere dynamics, due to the inadequate spatial resolution and the irregular observing schedules. A different observing strategy is needed, similar to that employed during the International Geophysical Year (IGY), and currently used in tropospheric meteorology. Specifically, observations need to be carried out with good time resolution (minutes) for significant periods of time (years) over chains of observatories separated by a few hundred kilometers, if the spatial and temporal morphology of space-weather phenomena is to be unraveled. *This approach has been called for in the National Research Council's Decadal Research Strategy [10], and is being pursued through the Distributed Array of Small Instruments (DASI) initiative.*

Figure 2 shows an ideal distribution of observatories with 100 km north-south spacing and 300 km east-west spacing. Sojka et al. [9] argued that this spacing should be considered minimal for resolving ionospheric structures and gradients, and for achieving the desired mesoscale D- and E-region specification. This grid would require about 90 observatories. The primary hurdle in establishing such an observing grid is, of course, economics. In order to establish a large observing grid, the cost of each observatory

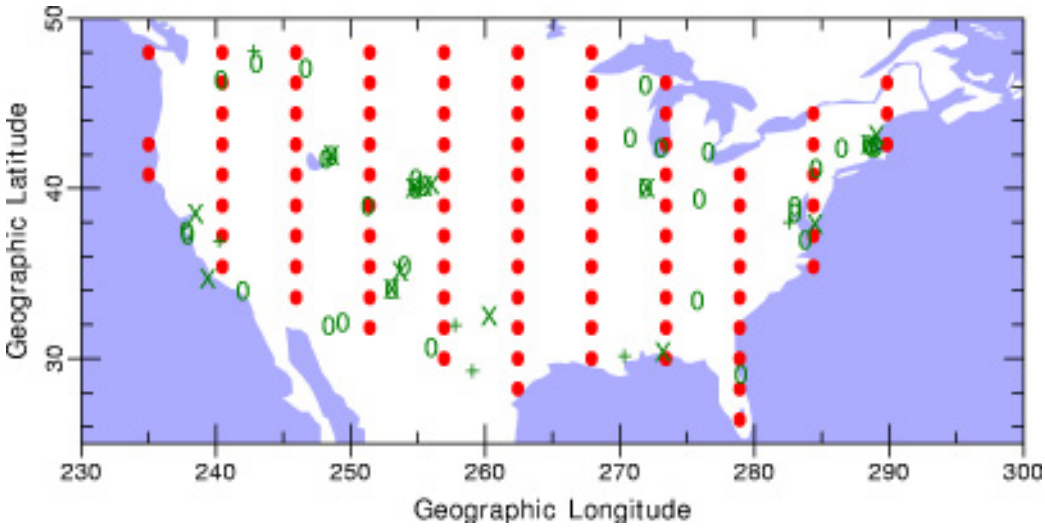

Figure 2. A minimal 100×300 km observation grid (red dots) covering the contiguous United States, compared to existing observatories (see Figure 1).

must be reasonable, and perhaps more importantly, the operating costs must be minimized. These constraints imply that each observatory must be physically small and have low maintenance, energy, and communications requirements.

One example of an extensive observation grid is the TEC (total electron content) mapping provided by dual-frequency GPS receivers. The Continuously-Operating Reference Stations (CORS) and International GNSS Service (IGS) networks provide detailed F-region information via TEC measurements. They are widely deployed across several continents, particularly in regions prone to earthquakes. The GPS instrument is relatively inexpensive, typically costing under US$20K. The networks are funded by many national agencies for various primary tasks, such as monitoring ground movements, providing accurate geolocation, and as aids to navigation. The space-weather application thus does not have to fully fund the establishment and operation of these networks.

A different approach has been demonstrated by SuomiNet (http://www.suominet.ucar.edu): rather than relying on instruments primarily dedicated to other uses, SuomiNet has established approximately 70 observatories in North America, and several on other continents, by working with schools and scientific organizations. Its observatories are small, PC-based units, with relatively sophisticated GPS receivers and meteorological sensors, which obtain various atmospheric parameters (including ionospheric TEC.) This network requires few resources, and the computer/GPS receiver can be set up in available space within existing buildings, minimizing setup costs. Local operations and maintenance (O&M) costs are minimal, since components use off-the-shelf technology. The result is a practical and cost-effective observing grid, yielding maps of TEC and meteorological quantities over wide areas with good temporal resolution.

We propose to use a similar approach to establishing observatories to map weather in the lower ionosphere. Our instrument, the Space-Weather-Aware Receiver Element (SWARE), uses software-defined radio (SDR) and a compact active antenna to monitor terrestrial beacons in the VLF through HF frequency range. Ionospheric- and propagation-modeling software is used to infer weather effects from observed signal-propagation characteristics with a temporal resolution of a few minutes. SWAREs can be set up in any location that provides computer power and Internet communications, and has low levels of radio-frequency interference (RFI). Most of the existing units are running in suburban residential environments.

Radio signal strength data from the SWARE network is collected and analyzed using comparisons to ionospheric-model and ray-tracing estimates. Data from other instruments, e.g., the low-power Canadian Advanced Digital Ionosonde (CADI) at the Bear Lake Observatory in Utah, and from other radio-propagation monitors, such as the amateur radio PropNET system (http://www.propnet.org), may also be used in the analysis. The primary products are D-region bottomside profiles and variability measurements obtained from VLF signal analysis; model D-region profiles augmented by HF absorption measurements; mesoscale sporadic E maps based on exceptional HF propagation and supported by ionogram analysis; and F-region variability measurements based on HF propagation observations compared to model estimates.

2. Passive Beacon Monitoring Revisited

Scientific studies based on passive monitoring of terrestrial radio beacons have been carried out on numerous occasions. Bixby [11] monitored the HF WWV signal (then transmitted from Washington, DC) to study HF propagation

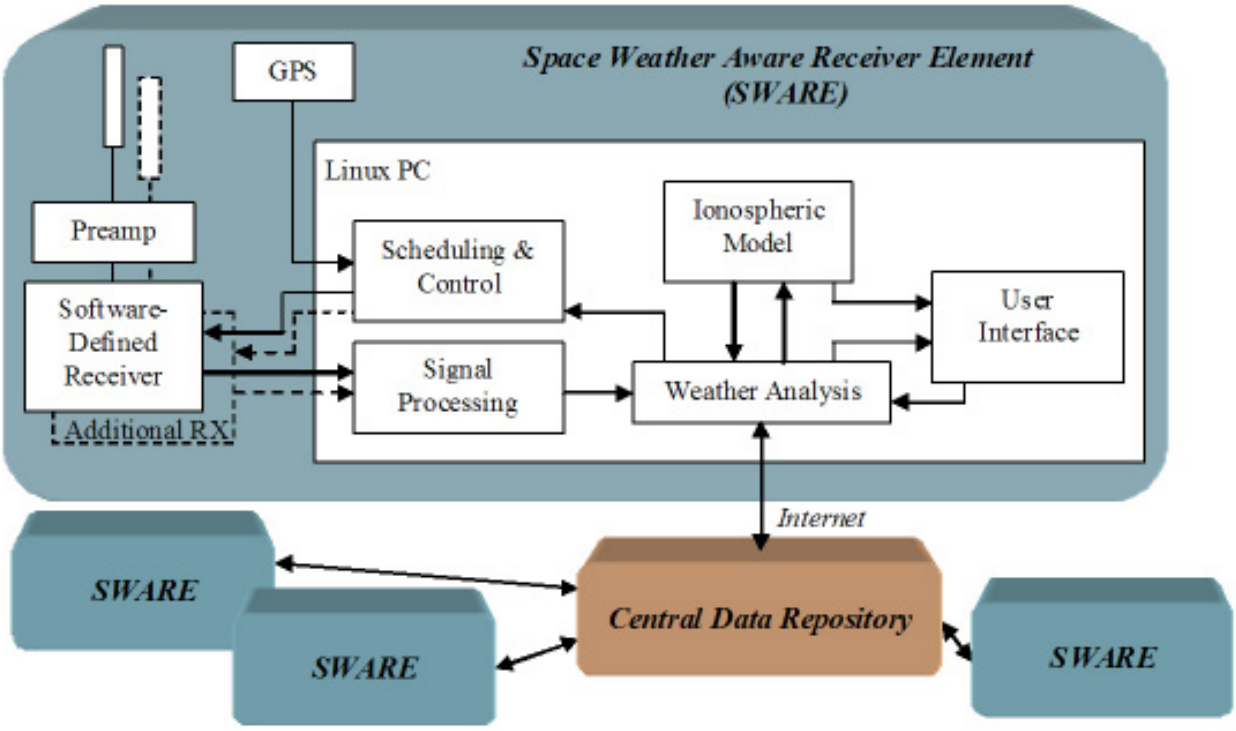

Figure 3. The Space Weather-Aware Receiver Matrix (SWARM), composed of Space Weather-Aware Receiver Elements (SWAREs) communicating with the Central Data Repository (CDR) via the Internet.

characteristics. Hunsucker [12, pp. 176-180], described oblique-incidence field-strength observations used to make absorption measurements in various frequency regimes. Definitive studies of the winter absorption anomaly were performed by Schwentek [5] using HF beacon monitoring. More recently, Navy VLF transmitters have been used as beacons to study D-region responses to solar flares and lightning (e.g., [4, 13-16]).

Traditional beacon studies have used one or a few frequencies during campaigns lasting for a few weeks or months. The limiting factor has been the interface between the radio receiver and the data acquisition and analysis equipment. Tuning to different beacons was difficult, and verifying that the received signal was due to the desired beacon and not from some other transmitter or interference generally required human oversight. These limitations are addressed by the modern software-defined-radio (SDR) receiver, which allows full computer control of all receiver functions and signal processing. Transmitters are chosen that have distinctive signals (such as the tone sequence used by WWV/WWVH) to allow the computer to determine the strength of the desired signal in the presence of noise and interference.

The Space Environment Corporation (SEC) began its passive beacon studies with the HF Investigation of D-region Ionospheric Variation Experiment (HIDIVE) and the Data Driven D-Region (DDDR) programs. Their goal was to obtain pertinent absorption data, and to ingest them to produce an improved D-region absorption model and HF propagation-prediction programs [17]. Most mid-latitude ionospheric D-region models and HF propagation-prediction programs include the solar zenith angle and the frequency-squared variation of absorption. However, the increased D-region absorption caused by specific space-weather effects, such as solar x-ray flares, changes in the neutral atmosphere, or storm-time auroral precipitation, are not included. Eccles et al. [18] described the HIDIVE and DDDR programs in detail, providing examples of ionospheric weather phenomena inferred from the HF signal observations.

The HIDIVE monitoring system implemented by Space Environment Corporation and RP Consultants began operation at the end of 2002, using an Icom R75 computer-controlled receiver to monitor all WWV/WWVH frequencies, in turn. While lacking the flexibility of the full SDR, the Icom interface was adequate to control the receiver and to acquire the signal-strength data from the receiver's automatic gain control. The audio signal was digitized and analyzed by the PC to determine relative signal-to-noise ratios. Radio monitors for the HIDIVE project were established at Bear Lake Observatory (BLO) in northern Utah; Providence, Utah (PRV); and Klamath Falls, Oregon (KFO.) These monitors demonstrated the ability of the simple HF monitor to make useful assessments of the propagation path, ionospheric absorption, and probable sporadic-E events.

New beacon monitors were designed in 2006 to cover a broader range of frequencies, and to support more-sophisticated data acquisition. The new beacon monitors

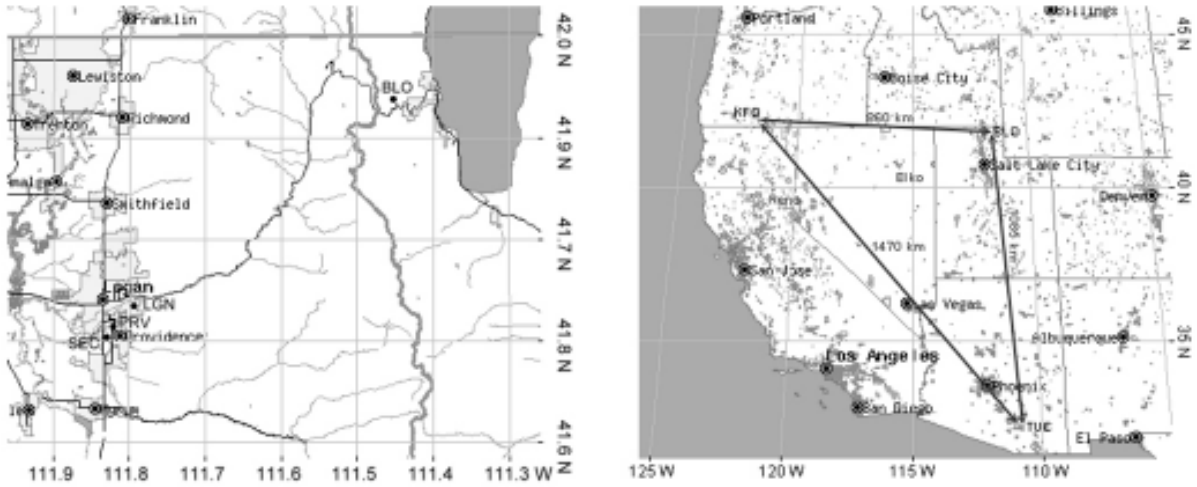

Figure 4. The initial SWARM deployment completed in November 2007, showing northern Utah (left) and the southwestern US (right). Shaded areas are populated regions. The cluster of systems in the Logan/Providence area is used for development and testing. In addition, field campaigns have been conducted at various locations in Oregon, Idaho, and Nevada.

were also given the task of performing some of the ionospheric and propagation modeling. The monitors thus became Space Weather-Aware Receiver Elements (SWAREs), and will be expected to take on more of the analysis load as the system evolves. The SWARE consists of a *Linux* PC outfitted with a winRadio G313i software-defined receiver, and a compact LF Engineering active antenna. A Garmin GPS receiver provides time and location information.

Each SWARE operates on a 15-minute duty cycle, averaging signal-strength measurements from the designated beacon transmitters, and estimating the noise in the receiver bandwidth. Each beacon signal is monitored for 10 seconds, according to a schedule that may be modified depending on conditions and observation objectives. Currently, five sets of average signal strengths are produced for each beacon in a 15-minute cycle. The SWARE also runs an ionospheric model to produce D-, E-, and F-region profiles for the area encompassing the receiver and all beacon transmitters, and performs ray-tracing through the model ionosphere for each HF signal at the 15-minute cadence. Waveguide-mode analysis of the VLF signals may also be performed. Discrepancies between observations and model analysis may indicate space-weather effects, as discussed in Sections 4 and 5.

The network of SWAREs is the Space-Weather-Aware Receiver Matrix (SWARM), depicted in Figure 3. A Central Data Repository (CDR), located at SEC, collects observations of beacon signal strength from the individual SWAREs, and also distributes geophysical indices, updates, and directives to the remote units.

The current SWARM deployment is shown in Figure 4. The three primary sites are at the Bear Lake Observatory (BLO) in northern Utah; Klamath Falls (KFO), Oregon, maintained by Dr. Robert Hunsucker; and Tucson (TUC), Arizona, maintained by Dr. John Raitt. These three locations form a triangle with an 860 km east-west alignment between BLO-KFO, and a 1,085 km north-south alignment between BLO-TUC. The baselines then provide the outer spatial mapping scale, 1,000 km, for the SWARM to study 10 to 1,000 km ionospheric structures.

Figure 5. The primary transmitter/receiver paths that are currently monitored. NPM and WWVH are in Hawaii.

Additional SWAREs have been deployed at other locations. Initial development sites were in River Heights (PRV), Utah; Providence (SEC), Utah; and in Logan (LGN), Utah. The separation distance between these three is less than 10 km, and the group lies about 40 km southwest of BLO. Currently, these SWAREs are being used in field-observation campaigns, lasting from a few days to a few months, at various locations in Idaho, Oregon, Nevada, and Montana. Deployments in western Canada are anticipated in 2009.

The primary VLF transmitters for the western United States are NML (25.2 kHz) in La Moure, North Dakota, and NLK (24.8 kHz) in Jim Creek, Washington, with relatively short transmitter-receiver paths. Longer paths to NAA (24.0 kHz) in Cutler, Maine, and NPM (21.4 kHz) in Lualualei, Hawaii, are also monitored, since they may help characterize large-scale phenomena. The paths are shown in Figure 5. Two HF transmitters – WWV in Ft. Collins, Colorado, and WWVH in Kekaha, Hawaii – are also monitored, continuing the HIDIVE observations. WWV and WWVH operate at 2.5, 5, 10, and 15 MHz; WWV also transmits on 20 MHz.

Plans call for the expansion of the number of transmitters being monitored as the acquisition and analysis software evolves. The number of signals available in the VLF range is limited, but there are a large number of potential LF beacons. The LF time-standard station WWVB (60 kHz) at Ft. Collins, Colorado, has recently been added to the monitoring sequence. Numerous aeronautical beacons operating in North America will be exploited to provide useful information about conditions in the lower ionosphere between dusk and dawn. At HF, amateur-radio beacons are

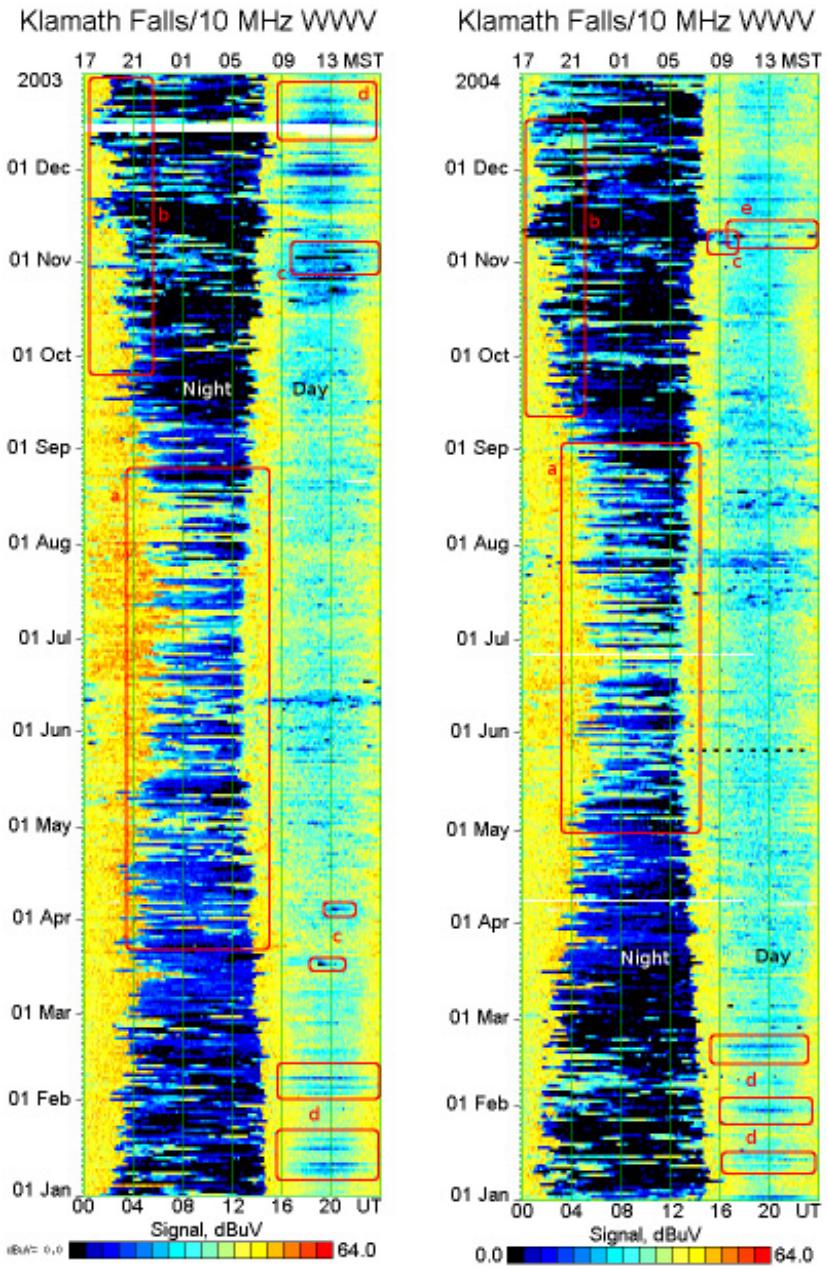

Figure 6. A comparison of the HF WWV 10 MHz signal received in Klamath Falls, Oregon, during 2003 (left) and 2004 (right.) The dark region in the center is night, when the MUF drops below 10 MHz for this path. Labels mark weather phenomena (see text).

the major source of widely-distributed transmitters. Extensive beacon networks already exist to allow amateurs to identify and exploit sporadic-E occurrences [19, 20]. Some HF amateur-radio observations are currently included in SWARE analyses.

3. Weather in the Lower Ionosphere

This study focuses on weather effects in the lower ionosphere, below about 150 km. Daytime electron density in this region ranges from about 10^5 electrons per cm^{-3} in the E region, to less than 100 per cm^{-3} at the bottom of the D region. During quiet conditions, the electron density of the lower ionosphere changes by at least two orders of magnitude over 24 hours. The best-known weather effect in this region is sporadic E, typically in the 90-120 km height range. This strongly reflects radio waves in the HF spectrum, and can provide over-the-horizon reflections up to about 100 MHz. However, there are also strong quasi-periodic variations in the D region, which cause variable daytime absorption of radio waves in the lower HF range. The D-region bottomside also controls VLF propagation, and even at night there is sufficient ionization below the E region to affect VLF. Thus, studies of VLF and HF signals can provide information about D-region variations, and HF signals may provide information about sporadic E.

Data collected by HIDIVE show numerous effects of D-, E-, and F-region weather, with observations spanning major space-weather storms. Figure 6 shows the signal strength on the WWV-KFO 10 MHz path for 2003-2004. White lines are missing data due to system downtime; the completeness of the data set demonstrates the reliability of the beacon-monitor hardware. The dark band in the middle of each panel is local night, when the maximum usable frequency of the path drops below 10 MHz. The left edge of the dark band is dusk, and the right edge is dawn. Notable weather effects are summarized below.

1. During summer, there is frequent propagation at night due to sporadic E. The presence of sporadic E on the WWV-KFO path is often confirmed by the CADI ionosonde, operated by SEC at Bear Lake Observatory, which is near the midpoint of the WWV-KFO path.
2. Major solar activity occurred late in both 2003 (the Halloween storm) and 2004. During these times, the dusk line was modulated with a 27-day period, corresponding to increases in F10.7 as the most active regions of the sun rotated into view.
3. Daytime short dark features that were black fading to gray (left-to-right) were solar X-ray flare absorption events. Examples of moderate flares were at 1900 UT on 17 March 2003, and 2000 UT on 4 April 2003. Large flares occurred at 2100 UT on 29 October 2003, 1800 UT on 2 November 2003, and 1600 UT on 7 November 2004.

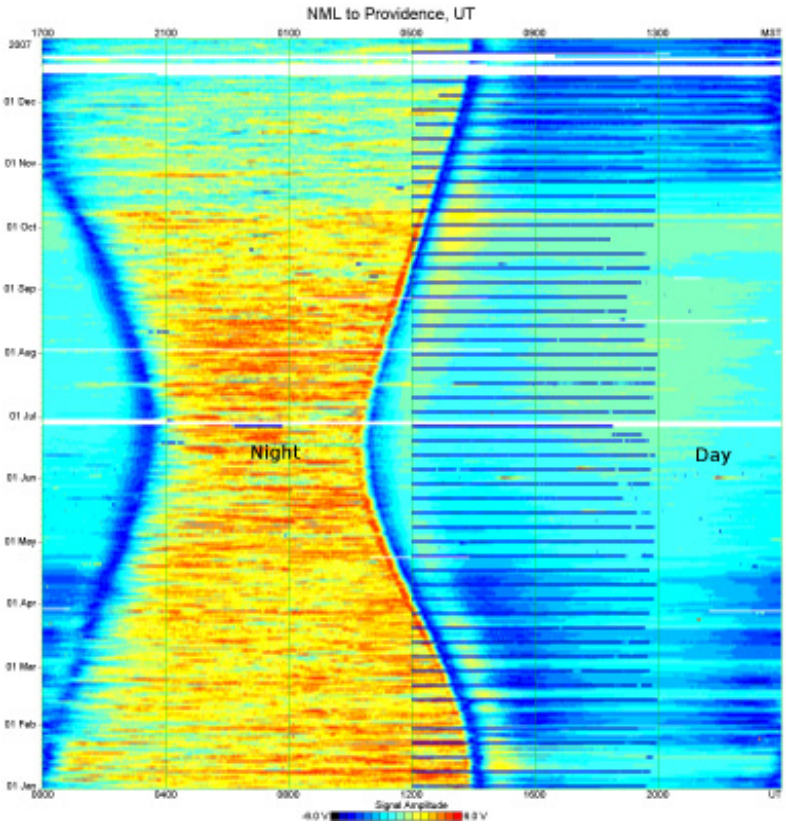

Figure 7. VLF signal strength observations for 2007 from the Stanford NML receiver (25.2 kHz) in Providence, Utah. Signal levels were typically higher and more variable at night than during the day.

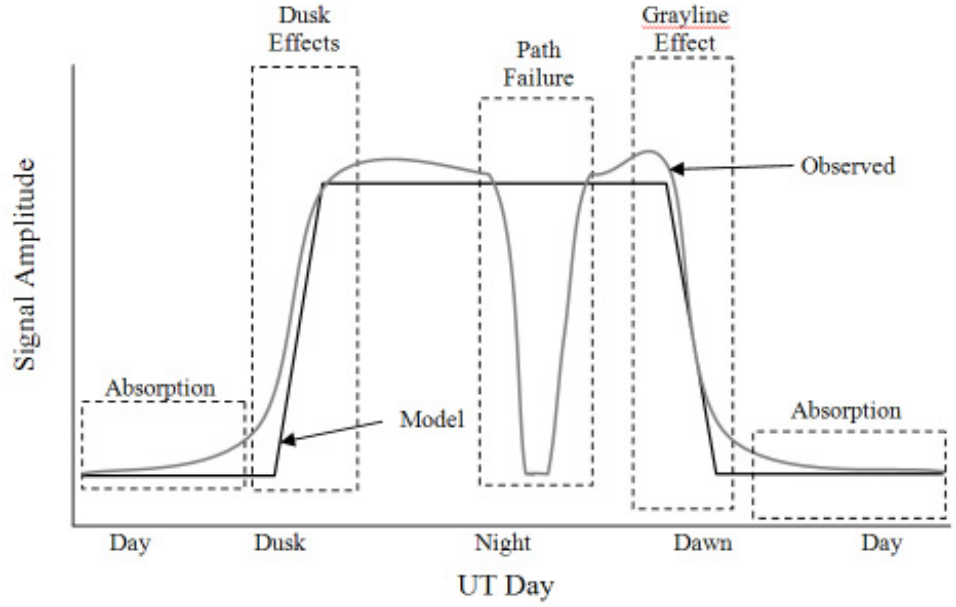

Figure 8. Low-HF propagation modeling and analysis. The daytime signal is completely absorbed and provides little information. The dusk-signal increase shows the complex interaction of D- and E-region decay and F-region lifting. At night, the power spectrum may reveal gravity-wave activity; a sharp drop indicates a path failure, either due to inadequate foF2 or sporadic E blocking the path. A dawn grayline signal enhancement is often observed before absorption eradicates the signal.

4. Daytime dark regions that lasted for more than one day were often winter-absorption anomalies. The anomalies were identified by a solar-zenith-angle dependence in the signal level, as shown below. Severe absorption was seen in early December 2003. Milder absorption anomalies could be seen in early January and February in both 2003 and 2004.
5. Other instances of low daytime signal (e.g., 10 November 2004) were associated with ionospheric storms that caused large fluctuations in F-region densities, and lowered the MUF below 10 MHz.

Some limitations in characterizing the D region by means of HF propagation analysis may be addressed by examining VLF propagation. For example, the nighttime D and E regions (other than sporadic E) have no significant effect on HF signals, but VLF is sensitive to the low nighttime densities at those heights. Another HF limitation is seen during large X-ray flares, where the normal daytime HF signals may be completely absorbed, while VLF signals change in interesting and sometimes complex ways.

VLF data collection began in conjunction with Stanford University's Sudden Ionospheric Disturbance (SID) project for the International Heliospheric Year (IHY), using dedicated single-frequency receivers with loop antennas. The complete 2007 VLF data set of the NML-to-Providence (PRV) path, obtained from the Stanford SID receiver, is shown in Figure 7. The very distinctive hourglass shape was due to the seasonal variation of daylight hours, similar to the dark region in Figure 6. The area inside the hourglass shape was nighttime, where maximum signal levels were usually observed for this path, and the narrowest section of the hourglass was summer solstice. The series of regularly-spaced black horizontal stripes between 1200 and approximately 2000 UT represented once-per-week maintenance outages of the NML transmitter. White areas were missing data, caused by failures at the receiver site. For this path, solar X-ray flares produced enhanced signals: three moderate flares could be seen in early June after 1400 UT, appearing as light streaks.

While the analysis of the HF signal depends primarily on the ability of the ionosphere to reflect or absorb the signal at a given time, the VLF signal strength depends on the interference between modes in the earth-ionosphere waveguide. For the NML-PRV path, analysis indicated a well-defined signal-strength minimum associated with an effective height of H′ ~84 km. Daytime H′ values were ~72 km, and nighttime values were ~90 km. Thus, at dawn and dusk, H′ passed through the minimum-signal region, producing the sharp border of the hourglass shape. The dawn crossing (right side) was sharper than the dusk crossing, and was sharpest in summer. This behavior was consistent with the solar zenith angle changing more rapidly during summer dawn than during winter dawn. The dusk crossing was indistinct at times during the winter, suggesting that the vertical gradients at dusk prevented the significant signal minimum from occurring.

Some seasonal effects in Figure 7 had less-obvious causes. Daytime signal levels increased abruptly in mid-April and decreased again in October. A gradual shift between winter and summer signal levels was expected due to higher summer sun angles, but the abrupt change suggested another cause, such as a seasonal change in mesospheric wind patterns. The nighttime signal levels reached much higher levels in the summer, but also had much greater

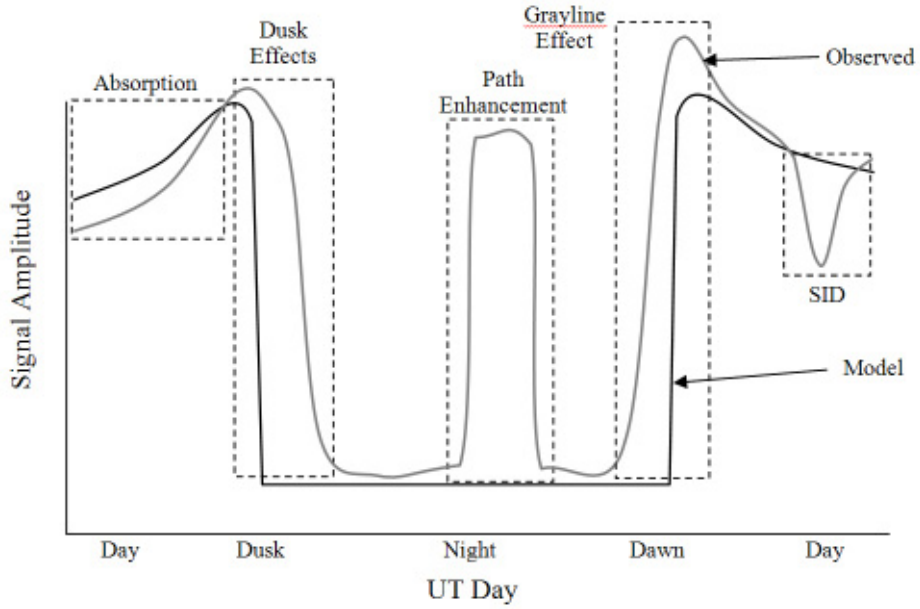

Figure 9. Mid-HF propagation modeling and analysis. The daytime signal is absorbed as a function of solar zenith angle and D-region NO concentration. At night, the signal exceeds the MUF, and propagation ceases. Occasionally, a path enhancement enables nighttime propagation. A dawn grayline enhancement is often seen. Solar flares increase D-region absorption and produce an HF SID signature.

variability, with nighttime signals erratically dropping below daytime levels. The greater summertime variability could be due to H′ being lower in summer than in winter, near the very sensitive range of H′ ~84 km, where the signal strength minimum occurred on the NML-PRV path. For a summer H′ ~ 87 km,, vertical motions due to winds and waves would produce larger signal variations than for a winter H′ of 90 km.

The behavior shown in Figure 7 was specific to the NML-PRV path. The seasonal behavior was actually quite similar in the NLK-PRV data, which had a similar path length. However, diurnal signal changes in KFO and TUC data were very different, due to differing Earth-ionosphere waveguide lengths and geometries. For example, the NLK-KFO data had a strong signal enhancement at dawn and dusk rather than a minimum, while NML-KFO, NML-TUC, and NLK-TUC paths had very subtle changes in signal levels at dawn and dusk.

4. HF Signal Data Analysis

Weather effects are inferred by comparison of measured signal levels to expected signal curves. For HF, the expected signal curve is derived from ray tracing through

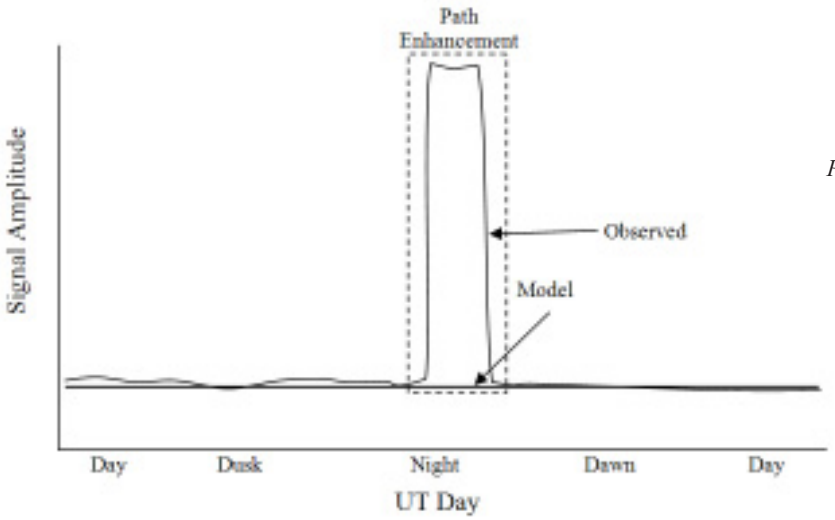

Figure 10. High-HF propagation modeling and analysis. The signal exceeds the MUF day and night. Propagation occurs occasionally due to a path enhancement, such as sporadic E.

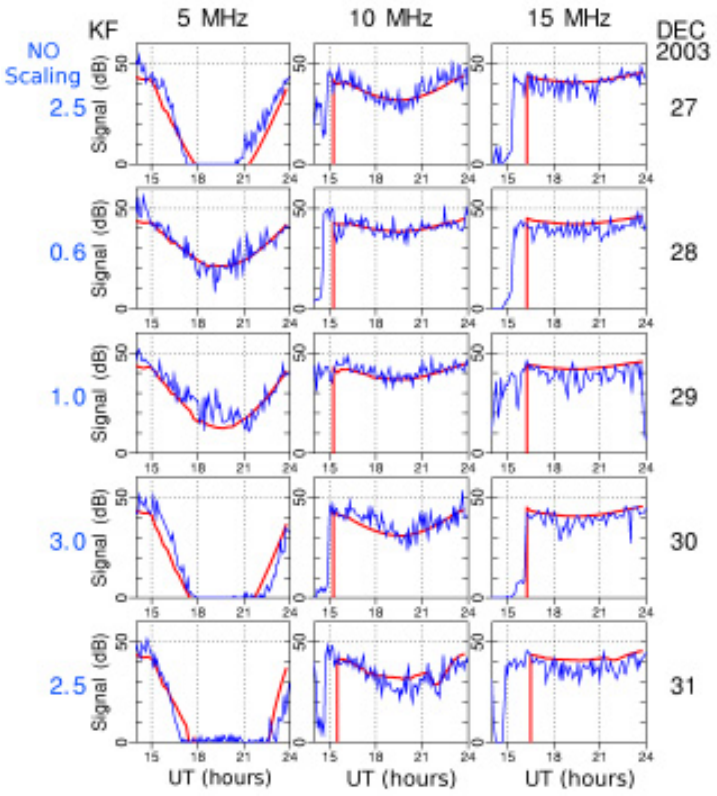

Figure 11. The KFO signal strength at 5, 10, and 15 MHz for December 27 through 31, 2003. The solid lines are the observed signal strength, while the dashed lines are the DDDR simulations based on scaled NO profiles, the scaling factors for which are listed at the left of each 5 MHz panel.

a model ionosphere. The median signal for the past week is used to establish the typical range of signal amplitudes.

The model ionosphere is produced by blending a D-region model (DDDR) with E- and F-region model results. The DDDR model is a simple ion-chemistry model of the D region, designed to incorporate sufficient positive and negative ion chemistry to generate an appropriate electron density for a wide range of natural geophysical conditions. Presently, the D-region model contains sufficient physics and chemistry to provide an electron density profile from 40 to 110 km altitudes for mid- and low-latitude HF propagation paths. The D-region model uses geophysical data streams available at NOAA, which provide real-time input into the space-weather events that affect D-region densities. The E and F regions may be modeled by a standard code such as IRI [21]. The results are combined to provide a complete electron-density specification for HF propagation and absorption calculations. The ray tracing is achieved using Dr. C. Coleman's HASEL ray-tracing program [22], modified to calculate path absorption.

HF paths for HIDIVE and SWARM are chosen so that single-hop E and F propagation is probable, and the signal behavior may be described by one of the following three cases.

First, low-HF paths have frequencies well below the typical MUF, generally below 10 MHz. As shown in Figure 8, the expected signal curve has strong nighttime propagation, but daytime signals are strongly absorbed. Weather effects are thus limited to dusk through dawn, and are largely controlled by F-region behavior. Periodic fades due to atmospheric waves are common, but at times path failure occurs. Path failure may be due to the MUF falling below the signal frequency, or due to sporadic E blocking the primary propagation path.

Second, mid-HF paths have frequencies below the daytime MUF, but above the nighttime MUF (Figure 9.) Measuring the depth of daytime absorption relative to the expected signal curve provides an estimate of D-region density variation. Sharp departures from the expected signal curve may indicate solar-flare absorption events. At night, a well-defined path enhancement may be due to an unexpected MUF increase or to sporadic-E propagation. A dawn enhancement is often observed, and propagation may resume somewhat earlier than the expected signal curve indicates, due to focusing effects.

Third, high-HF paths have frequencies well above the MUF, generally above 15 MHz. In this case, the expected signal curve is always at the noise floor (Figure 10.) If the signal frequency is sufficiently above the MUF, path enhancements are generally assumed to be due to sporadic E.

The primary phenomena of interest for mapping are sporadic E and absorption. Sporadic E may be inferred from path enhancements in nighttime mid-HF paths and all high-HF paths when MUF variations are judged inadequate to produce the path enhancement. Absorption is obtained from daytime mid-HF paths.

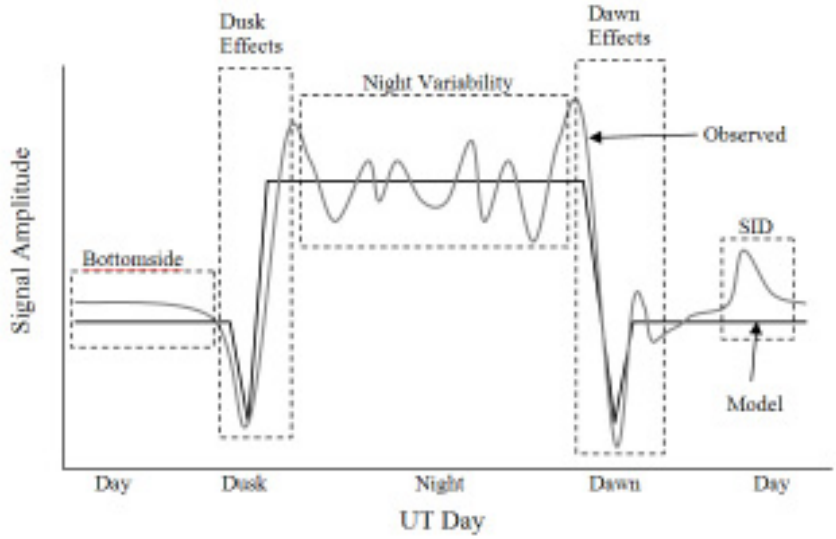

Figure 12. VLF propagation modeling and analysis. The daytime signal provides the D-region bottomside profile (left), while SID signature detection (right) allows the D-region enhancement from a solar flare to be estimated. Dawn and dusk effects allow the rate of change of the D-region profile to be quantified. Dawn often includes focusing that is not well modeled. At night, variability (average, standard deviation, power spectrum) indicates the level of atmospheric disturbance (winds and waves) at about 90 km.

Figure 11 shows an example of winter absorption changes observed by HIDIVE on a mid-HF path in December 2003, and analyzed with DDDR. For the multiple daytime scale shown, the D-region variability responsible for the changes in absorption was thought to be associated with redistribution of the mesospheric NO via planetary waves [6]. The changes in absorption were thus addressed by changing the NO concentration in the D-region model.

Large day-to-day variability of 5, 10, and 15 MHz WWV signals received at Klamath Falls was observed from December 27 to 31, 2003. The effect was most noticeable on the 5 MHz signal. Signal strength on December 27, 30, and 31 fell too low to be detected at noon (around 1900 UT), while on December 28 and 29, the absorption was at least 20 dB less. In order to model these differences, the NO level for each day was scaled. On the three strong absorption

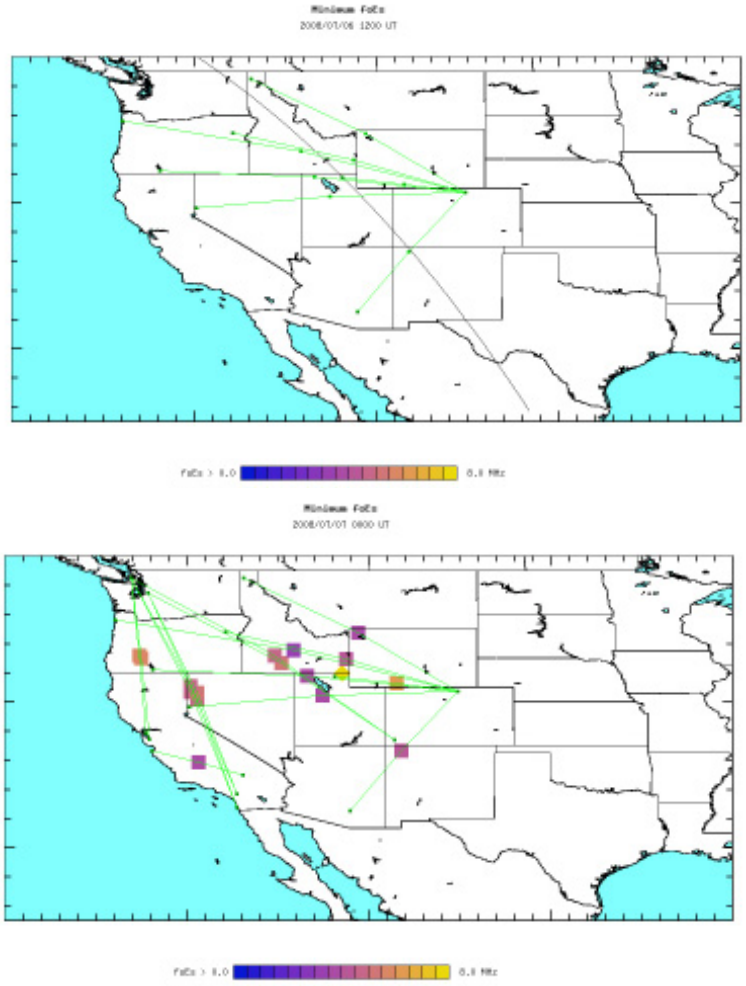

Figure 13. Sporadic-E minimum densities mapped during July 2008. No sporadic E was detected at 1200 UT on 6 July 2008 (top), but twelve hours later, sporadic E was present across the western US (bottom). The curved line in the top map was the dawn terminator. SWARE HF paths originated with WWV in Ft. Collins, CO. Other paths involved amateur-radio HF beacons.

days, factors of 2.5, 3.0, and 2.5 were needed on December 27, 30, and 31, respectively. On December 28, a reduction in NO was required, i.e., a factor of 0.6. The same factors were used for 10 and 15 MHz. The NO factor on various paths may be used to develop a map of D-region variations.

5. VLF Signal Data Analysis

At VLF, an expected signal curve is developed based on a different modeling strategy. Instead of ray tracing, the appropriate propagation model for these longer wavelengths is a waveguide defined by the Earth below, and bounded above by the D region. This analysis is performed by the US Navy's Long Wave Propagation Capability (LWPC) [23], which has been used for many other scientific studies. An exponential ionosphere defined by effective height and slope parameters is used to describe the bottom of the D region, in conjunction with DDDR for LWPC. The median signal level of the past week is used to set the range of signal levels.

The shape of the expected signal curve varies dramatically with the path. Figure 12 shows a curve typical of NLK or NML received in northern Utah. During the day, variations from the expected signal allowed the exponential bottomside parameters to be adjusted; these changes were typically small. More dramatic changes were inferred from SID signatures, when the bottomside effective height dropped significantly and the D-region density increased. At night, the variability of the signal is quantified by the mean and standard deviation, and atmospheric wave activity is quantified by power spectra. The rate of change of dawn and dusk signals is used to determine the change in the D-region effective height.

The VLF analysis thus far has led to modifications of the D-region model's nighttime chemistry, as well as preliminary inversions of X-ray flare SIDs and winter-anomaly enhancements.

6. Data Mapping

When multiple-sensor observations are combined, information about the spatial characteristics of the ionosphere may be deduced. In Figure 13, the minimum sporadic-E critical frequency required to provide observed HF propagation was mapped for two times in the western United States. Observations included SWARE 20 MHz WWV signal strength, ionograms from the Bear Lake Observatory in Utah, and HF amateur-radio beacon-signal observations. In the first instance (top panel), no sporadic-E propagation was observed for any monitored path. Sporadic-E observations increased during the next twelve hours, until it was observed on most of the monitored paths (bottom panel.)

The maps produced by the prototype network, though sparse, have demonstrated the complexity of the sporadic-E phenomenon summarized by Whitehead [7]. During the summer, sporadic E was observed to appear almost simultaneously across the monitored paths in the western United States, "blooming" in a manner reminiscent of summer thunderstorms on weather maps. A few instances were found where sporadic E appeared to travel across the mapped area: on 4 July 2008, sporadic-E propagation spread westward with an apparent motion of 68 m/s. Some sporadic-E maps indicated broad bands with northern and southern boundaries, while others showed clouds limited in both latitude and longitude. During the summer, regular morning and evening sporadic-E events were noted, similar to the semi-diurnal tide effects described by Mathews [24]. A prolonged series of sporadic-E events were observed in late 2008 with a regular 24-hour pattern.

Currently, efforts are being made to map D-region variations related to the winter-absorption anomaly. These events have been less dramatic during the period of SWARE operation, due to the unusually-quiet solar-minimum conditions. However, there is some indication of connections between daytime D-region absorption at HF and nighttime VLF signal fluctuations suggestive of an equator-ward drift. More observations of these effects are needed.

7. Conclusion

The Space Weather-Aware Receiver Element (SWARE) has been designed to monitor ionospheric conditions and signal-propagation characteristics with good time resolution (<15 minutes) and minimal cost. Affordability includes not only the initial cost of the instrument, but also the small footprint, high reliability, and low operation and maintenance costs.

The SWARE provides real-time raw signal and initial model results to the local operator. When combined with other units to form a Space Weather-Aware Receiver Matrix (SWARM), the results can be turned into a geographical map of the observed and modeled parameters covering thousands of kilometers, with resolution on the order of 100 km. Observations from other instruments and observation networks may be ingested into the mapping process. The comparison of observations at the Central Data Repository (CDR) also allows for better quality control, isolating anomalies that may be due to local interference or equipment failures. The current development emphasis of the signal data analysis is to create the following products:

- D-region structure specification in latitude and longitude, including the absolute density profile from the Data-Driven D-Region model. This will improve HF radiowave absorption determination, as well as defining the upper boundary conductivities for waveguide propagation calculations below 1 MHz.

- E-region structure specification in latitude and longitude, with a particular emphasis on sporadic-E conditions for operational users and scientific studies. The primary goal is to map the mesoscale spatial distribution of sporadic E, setting bounds on the sporadic layer density.

- F-region variation specification in latitude and longitude through modeling with observational bounds on the profile's peak density.

Efforts are underway to improve observations with additional SWARE sites in the western United States and Canada. Data acquisition, modeling, and analysis software are evolving steadily, with current data and analysis results available at http://www.spacenv.com/~agile.

8. Acknowledgement

This research was supported by SBIR II contract FA8718-07-C-0016 from AFRL at Hanscom AFB to Space Environment Corporation. The VLF SID Space Weather Monitor is an instrument developed through a project sponsored by Stanford University, the National Science Foundation, NASA, and is part of the United Nations' International Heliospherical Year, 2007. See http://sid.stanford.edu for project information and data. We also wish to acknowledge the contribution of many radio amateurs through the PropNet project (http://www.propnet.org).

9. References

1. B. V. Khattatov et al., "Dynamics of the Mesosphere and Lower Thermosphere as Seen by MF Radars and by the High-Resolution Doppler Imager/UARS," *J. Geophys. Res.*, **101,** D6, 1996, pp. 10,393-10,404.

2. K. D. Davies, *Ionospheric Radio*, London, Peter Peregrinus Ltd., 1990.

3. R. D. Hunsucker and J. K. Hargreaves, *The High-Latitude Ionosphere and its Effects on Radio Propagation*, Cambridge, Cambridge University Press, 2003.

4. W. M. McRae and N. R. Thomson, "Solar Flare Induced Ionospheric D-Region Enhancements from VLF Phase and Amplitude Observations," *J. Atmos. Solar-Terr. Phys*, **66**, 2004, pp. 77-87.

5. H. Schwentek, "Some Results Obtained from the European Cooperation Concerning Studies of the Winter Anomaly in Ionospheric Absorption," in K. Rawer (ed.), *COSPAR Proceedings of the Methods of Measurements and Results of Lower Ionosphere Structures Symposium held in Constance, F.R.G*, 1974, pp. 281-286.

6. K. Kawahira, "The *D* Region Winter Anomaly at High and Middle Latitudes Induced by Planetary Waves," *Radio Science*, **20**, 1985, pp. 795-802.

7. J. D. Whitehead, "Recent Work on Mid-Latitude and Equatorial Sporadic-E," *J. Atmos. Terr. Phys.*, **54**, 1989, pp. 401-424.

8. C. Haldoupis, D. Pancheva, and N. J. Mitchell, "A Study of Tidal and Planetary Wave Periodicities Present in Midlatitude Sporadic E Layers, *J. Geophys. Res.*, **109**, 2004, A02302, doi:10.1029/2003JA010253.

9. J. J. Sojka, D. Rice, J. V. Eccles, F. T. Berkey, P. Kintner, and W. Denig, "Understanding Midlatitude Space Weather: Storm Impacts Observed at Bear Lake Observatory on 31 March 2001," *Space Weather*, **2**, 2004, S10006, doi:10.1029/2004SW000086.

10. National Research Council, *The Sun to the Earth — and Beyond*, Washington, DC, National Academies Press, 2003.

11. L. H. Bixby, *Interpretation of WWV and WWVH Signal Strength Variations at Stanford*, PhD Dissertation, Stanford University, 1956.

12. R. D. Hunsucker, *Radio Techniques for Probing the Terrestrial Ionosphere*, New York, Springer-Verlag, 1991.

13. W. M. McRae and N. R. Thomson, "VLF Phase and Amplitude: Daytime Ionospheric Parameters, *J. Atmos. Solar-Terr. Phys*, **62**, 2000, pp. 609-618.

14. N. R. Thomson and M. A. Clilverd, "Solar Flare Induced Ionospheric D Region Enhancements from VLF Amplitude Observations, *J. Atmos. Solar-Terr. Phys.*, **63**, 2001, pp. 1729-1737.

15. N. R. Thomson, C. J. Rodger, and M. A. Clilverd, "Large Solar Flares and their Ionospheric D Region Enhancements," *J. Geophys. Res.*, **110**, 2005, A06306, doi: 10.1029/2005JA011008.

16. N. R. Thomson, M. A. Clilverd, and W. M. McRae, "Nighttime Ionospheric D Region Parameters from VLF Phase and Amplitude," *J. Geophys. Res.*, **112**, A07304, 2007, doi: 10.1029/2007JA012271.

17. J. J. Sojka, D. Rice, and J. V. Eccles, "Affordable Software Radio: A New Tool for HF Science and Space Weather Operations," 2005 Ionospheric Effects Symposium, 2005, pp. 254-263.

18. J. V. Eccles, R. D. Hunsucker, D. Rice, and J. J. Sojka, "Space Weather Effects on Midlatitude HF Propagation Paths: Observations and a Data-Driven *D*-Region Model," *Space Weather*, **3**, 2005, S01002, doi:10.1029/2004SW000094.

19. J. G. Troster and R. S. Fabry, "The NCDXF/IARU International Beacon Project: Report and Update," *QST*, **81**, 9, 1997, p. 47.

20. S. Ford, "PropNET," *QST*, **92**, 3, 2008, p. 95.

21. D. Bilitza, "International Reference Ionosphere 2000," *Radio Science*, **36**, 2001, pp. 261-275.

22. C. J. Coleman, "A General Purpose Ionospheric Ray Tracing Procedure," Rep. No. SRL0131TR, Defence Science and Technology Organisation, Australia, 1993.

23. K. Ferguson, "Computer Programs for Assessment of Long-Wavelength Radio Communications, Version 2.0," Technical Document 3030, May 1998, Space and Naval Warfare Systems Center, San Diego, CA 92152-5001 USA, 1998.

24. J. D. Mathews, "Sporadic E: Current Views and Recent Progress, *J. Atmos. Solar-Terr. Phys.*, **50**, 1998, pp. 413-435.